



## Abstract

A ~400 ka (kilo years) supra-Milankovitch cycle, recorded in the sodium, magnesium, lead, nickel and cobalt contents of a 32 mm thick ferromanganese crust from Vityaz fracture zone, central Indian ridge is reported here. To arrive at the geological ages, we used both  $^{230}\text{Th}_{\text{excess}}$  and Co-chronometric datings. The correlation coefficient between the  $^{230}\text{Th}_{\text{excess}}$  based dates and Co-chronometric dates for the top 0–8 mm is very high ( $r=0.9734$ , at 99.9% significance). The cobalt chronometric age for the bottom most oxide layer of this crust is computed as 3.5 Ma. Red-fit and multi-taper spectral analyses of time series data revealed the existence of the significant ~400 ka cycle, representing the changes in the hydrogeochemical conditions in the ocean due to the Earth's orbital eccentricity related summer insolation at the equator. This is the first report of such cycle from a hydrogenous ferromanganese crust from equatorial Indian ocean.

## 1 Introduction

Hydrogenous ferromanganese crusts are slowly grown ferromanganese (Fe-Mn) coating on hard substrates on top of abyssal hills, slopes and mountain flanks. These hydrogenous crusts are geologically stable and move with the substratum, but they record the hydrogeochemical history of the surrounding water column during their entire growth process. Earlier, the geochemical study of the Fe-Mn crust from the Indian Ocean Ridge system has been reported by Nath et al. (1997), Kuhn et al. (1998), and Herzig and Pluger (1998), wherein the crust formation processes are described and discussed in detail, but without any time series analyses. Herein, besides reporting the general geochemical variation in crust micro-layers, we attempted to understand their cyclic/acyclic nature during the time of elemental deposition in the geological past. Present crust location, the Vityaz fracture zone, central Indian ridge, lies beneath the high productivity equatorial region (Berger et al., 1989). It can be anticipated that this

CPD

6, 1311–1335, 2010

## A ~400 ka supra-Milankovitch cycle in a Fe-Mn crust

R. Banerjee et al.

Title Page

Abstract

Introduction

Conclusions

References

Tables

Figures

◀

▶

◀

▶

Back

Close

Full Screen / Esc

Printer-friendly Version

Interactive Discussion



location has been moved/readjusted from its original location within 2° (~200 km) south with respect to its present position, considering ~1mm/year northern movement of the Indian plate from Capricorn plate (DeMets and Royer, 2003) since the emergence of Himalayas during the late Miocene (Edwards and Harrison, 1997; Royer et al., 1997).

The Milankovitch cycles at ~100-, ~41-, and ~23-ka due to the Earth's orbital eccentricity, axial tilt and precession of equinoxes, respectively, are reported earlier in the Indian Ocean sediments (Hays et al., 1976; Gupta 2002, 2003). Recent studies also reported a supra Milankovitch ~400-ka eccentricity cycle in the climatic proxies like radiolarians and transfer function based sea surface temperature from the Indian Ocean (Gupta et al., 1996; Gupta, 2003), foraminiferal  $\delta^{18}\text{O}$  record from ODP site 607 in the North Atlantic (Clemens and Tiedemann, 1997), and the foraminiferal sand fraction of the ODP site 806 in the Western Pacific Ocean (Muller and Macdonald, 1997a,b). However, so far there is no report available regarding the existence of a ~400 ka supra-Milankovitch cycle in the geochemical climatic proxy records from the Indian ocean. In view of this, an attempt was made to study a slowly accreting hydrogenous ferromanganese crust from the equatorial Indian ocean, to trace the records of such long term climatic changes hidden in the elemental compositions of the finer layers of the crust. Although, the existence of "Milankovitch cycle" in a nodule (unoriented?) has already been reported by Han et al. (2003), here we report the existence of "Supra-Milankovitch" cycle in a very well oriented ferromanganese crust, not reported so far from any where from similar sample.

## 2 Sample and methodology

A 32 mm thick Fe-Mn crust was collected from the Vityaz fracture zone, central Indian ridge (5°34' S, 67°53' E; water depth, ~3500 m, Fig. 1). The crust sample has a 15 cm thick calcareous substrate, on top of which the ferromanganese coating has formed. Thus there is no difficulty to understand the top and bottom of the crust, which is later substantiated by studying their micro growth textures using their polished sec-

CPD

6, 1311–1335, 2010

### A ~400 ka supra-Milankovitch cycle in a Fe-Mn crust

R. Banerjee et al.

Title Page

Abstract

Introduction

Conclusions

References

Tables

Figures

◀

▶

◀

▶

Back

Close

Full Screen / Esc

Printer-friendly Version

Interactive Discussion



tions under reflected light microscope. The crust substrate has already been studied biostratigraphically and the results are published elsewhere (Guptha et al., 2002). The biostratigraphic age of the substrate was thus determined as early Pliocene (~3.7 Ma).

The crust with well preserved columnar and laminar growth patterns at different depth sections was analyzed by using a Electron Probe Micro Analyser (EPMA) following the method as described in Banerjee et al. (1999). For this, a JEOL-JXA 733 model EPMA was used with accelerating voltage of 15 kV, specimen current of 0.02 nA and electron beam diameter between 2 and 5  $\mu\text{m}$ . Synthetic oxide standards were used before measurement and the data were corrected using a ZAF programme. Similar method is also used in several other studies (Hein et al., 1992; Jeong et al., 2000) on millimeter level geochemical investigations of ferromanganese crusts and subsequently their age was determined by cobalt chronometry method. In order to understand the millimeter level geochemical variations a crust section was analyzed from outermost to innermost oxide layer, at every 100  $\mu\text{m}$  interval for 17 elements (Fe, Mg, Na, Al, Si, K, Ca, Ti, Mn, Ni, Cu, Co, Zr, Sr, Ba, Pb, Cr) and then averaged at each millimeter level (Table 1).

The crust was then dated using  $^{230}\text{Th}_{\text{excess}}$  (Banakar and Borole, 1991) and Co-geochemistry (Frank et al., 1999; Ren et al., 2007; Manheim and Lane-Bostwick, 1988; Puteanus and Halbach, 1988). As  $^{230}\text{Th}_{\text{excess}}$  based dates can not be derived with a high level of confidence in samples older than 0.5 Ma because of isotope half life limitation, this method could not be utilized for dating the entire crustal thickness of 32 mm. However, the correlation coefficient between the  $^{230}\text{Th}_{\text{excess}}$  based dates (Table 2) and Co-chronometric dates for the top 0–8 mm is very high ( $r=0.9734$ , at 99.9% significance level, Fig. 2), and it suggests that both the methods produced very high level of similarity in dating the datum level in the top layer of crust (0–8 mm). Therefore, our age model is constrained and dependent on Co-chronometric dates in samples below 8–32 mm of the crust. Using Co-chronometry (Frank et al., 1999; Ren et al., 2007; Manheim and Lane-Bostwick, 1988; Puteanus and Halbach, 1988) the age of the bottom most layer of the crust was calculated as ~3.5 Ma. Mixed-depth age

## A ~400 ka supra-Milankovitch cycle in a Fe-Mn crust

R. Banerjee et al.

Title Page

Abstract

Introduction

Conclusions

References

Tables

Figures

◀

▶

◀

▶

Back

Close

Full Screen / Esc

Printer-friendly Version

Interactive Discussion



model (Heegaard et al., 2005) was applied to ascertain the error limits in the computed age of the crust layers (Fig. 1). Later, time series of Na, Mg, Pb, Ni and Co in the crust was generated using the cobalt chronometric dates (Fig. 3a–e).

## 2.1 Cobalt chronometry

5 The Co-chronometer method (initially proposed by Manheim, 1986; and later elaborated by Manheim and Lane-Bostwick, 1988) adopted here is a highly recommended method for dating the deeper water ferromanganese crusts (>3000 m water depth), having a lower Co concentration of <8%, and of relatively younger age (<10 Ma) (Frank et al., 1999; O’Nions and Frank, 2000; Klemm et al., 2005). Calibration of the Co-chronometer and isotopic dating method using  $^{10}\text{Be}/^9\text{Be}$ , in case of growth rate and age determination of above mentioned type of ferromanganese crusts from several oceanic environments, with specific limitations, has already been discussed in detail by Frank et al. (1999), beyond any doubt. We have adopted similar method without jumping out of the prescribed limitations, to determine the age of the microlayers of the present ferromanganese crust sample. Interestingly, the bottom most age of the oxide layer determined by Co-chronometer method (~3.5 Ma) corroborates well with the earlier determined biostratigraphic age of it’s substrate (~3.7 Ma), as mentioned in the earlier paragraph.

## 2.2 Radio-isotopic dating

20 For this, scrapped and weighted sample from each successive millimeter of the crust was dissolved in 30 ml of 8 M  $\text{HNO}_3$  in the presence of  $^{232}\text{U}/^{228}\text{Th}$  spike. U-Th radio-chemical separation and purification were carried out following standard procedures (after Krishnaswami and Sarin, 1976). The alpha activity of the electroplated samples were assayed using ion implanted detector coupled to Octet plus Alpha spectrometer.

25 The error quoted are the cumulative error due to counting statistics. Table 2 summarizes the results of the radiometric analysis including the error limits.

### A ~400 ka supra-Milankovitch cycle in a Fe-Mn crust

R. Banerjee et al.

Title Page

Abstract

Introduction

Conclusions

References

Tables

Figures



Back

Close

Full Screen / Esc

Printer-friendly Version

Interactive Discussion



## A ~400 ka supra-Milankovitch cycle in a Fe-Mn crust

R. Banerjee et al.

Title Page

Abstract

Introduction

Conclusions

References

Tables

Figures

◀

▶

◀

▶

Back

Close

Full Screen / Esc

Printer-friendly Version

Interactive Discussion



The average  $^{234}\text{U}$  activity is  $(4.92 \pm 0.30)$  dpm/g. The values for  $^{230}\text{Th}_{\text{excess}}$  (excess  $^{230}\text{Th}$  is that portion of the  $^{230}\text{Th}$  which is not supported by the decay of  $^{234}\text{U}$  in the sediments) were calculated by subtracting the  $^{234}\text{U}$  activity from the total  $^{230}\text{Th}$  activities. The  $^{230}\text{Th}_{\text{excess}}$  is computed from the following equation.

$$^{230}\text{Th}_{\text{excess}} \text{ (dpm/gm)} = ^{230}\text{Th} \text{ (dpm/gm)} - ^{234}\text{U} \text{ (dpm/g)} \quad (1)$$

The cumulative inventory of  $^{230}\text{Th}_{\text{excess}}$  is calculated using the relation:

$$I \text{ (dpm/cm}^{-2}\text{)} = \int_0^{\alpha} A(z) dz = A_0 \rho S \tau k \quad (2)$$

where,  $A_0$ =extrapolated activity at the surface (361 dpm/g),  $S$ =growth rate cm/y ( $0.576 \times 10^{-6}$ ),  $\tau$ =the radioactive mean life ( $1.085 \times 10^5$  yr) of  $^{230}\text{Th}$ ,  $\rho$ =in situ bulk density ( $2.5 \text{ g/cm}^3$ ),  $k$ =a geometric factor=1 (for a rectangular geometry here).

The measured cumulative deposition of  $^{230}\text{Th}_{\text{excess}}$  in the crust ( $60 \text{ dpm/cm}^2$ ) is just 6% of its inventory ( $\sim 1000 \text{ dpm/cm}^2$ ) in the overlying water column. This observation is similar to the one reported by Banakar and Borole (1991) for a dep-sea crust from central Indian basin. This also corroborates the earlier findings that the growth of the crust is episodic and not continuous (Krishnaswami et al., 1973).

The  $^{230}\text{Th}_{\text{excess}}$  activity depth profile is shown in the inset of Fig. 1. The top 4 points (0–2 mm) shows a linear decrease with depth. Assuming the constant flux model (Koide et al. 1973; Krishnaswami and Lal, 1978) and constant initial concentration, the observed decrease is due to the radioactive decay of  $^{230}\text{Th}_{\text{excess}}$  and the deduced growth rate is  $(5.9 \pm 0.24) \text{ mm/Ma}$  ( $n=4$ ,  $p \leq 0.001$ ). While the remaining depth (2 to 8) mm yields a faster growth rate of  $(72 \pm 17.4) \text{ mm/Ma}$ .

### 3 Results and discussion

We have used RED-FIT (Schulz and Mudelsee, 2002) spectrum with critical algorithm setting of false-alarm level (Thomson, 1982) and scaling factor (2.35) for red noise

(r-test within critical values) in spectral analyses to rule out the red-noise process because of non-equidistal time interval ( $\delta t$ ) due to non-uniformity in the growth history (Fig. 1). The Na, Mg, Pb, Co and Ni qualified stringent criterion (Ofac 8, Hifac 1, and Welch window, Monte Carlo simulation 20000,  $\delta t=110$  Ka, 6-dB=0.2) of Red-fit settings, and resulted in significant cycles with  $\geq 90$ –95% Chi<sup>2</sup> test for the level of significance. Incidentally, sampling interval ( $\delta t$ ) at 110-ka data ruled out the aliasing effect (large sampling interval of a lower cycle generating a larger artifact cycle) by the 23-ka, 41-ka and 100-ka climatic signal to falsely generate the 400-ka eccentricity cycles of Berger (1978), and is dissussed later. Red-fit spectral results of the Na, Mg, Pb, Ni and Co suggested significant ( $\geq 90$ –95%)  $\sim 400$ -ka cycle (Fig. 4). This cycle is further verified by multi-taper method (MTM) of Thomson (1990), Mann and Lee (1996), and Ghil et al. (2001) by using SSA-MTM program-kit by Kondrosow (<http://www.atmos.ucla.edu/tcd/ssa/>). We employed red noise null hypothesis, high resolution spectrum, 50% reshaping thrushold, either (narrowband/normal) signal assumption, normalization, raw noise setting, and log-fit criterion in the MTM analyses (Figs. 5–7). Thereafter, we identified significant (90–95%) cycles in the MTM spectral power, and reconstructed the significant cyclic component comparing with the original time series data, which further substantiated the existence of the  $\sim 400$ -ka cycle in the Mg, Ni and Co records (Fig. 5). Recently, Hyun et al. (2005) reported  $\sim 400$ -ka cycle in the carbonate and the terrigenous contents of the K, Al, Ti, and Th variations in a geological record of last  $\sim 1$  Ma from the ODP Site 983 in the North Atlantic Ocean. Similarly, in our crust Na might have derived from similar sources. Eolian dust entering into ocean (Clemens, 1998) and its records from ODP-721-722 in the Arabian Sea (DeMenocal, 1995) and African monsoon dust records from ODP-659 in tropical Atlantic off West Africa (Tiedemann et al., 1994) derived by monsoon winds suggested that monsoon enhanced at  $\sim 400$ -ka eccentricity maximum and weakened at its minimum signals in the Plio-Pleistocene time. Similarly, the magnetic susceptibility data from ODP Hole 821A recovered from the Great Barrier Reef in the Pacific Ocean exhibited the  $\sim 400$ -ka cycles in a  $\sim 1.5$  Ma record of the mixed silici-clastic and carbonate

---

## A $\sim 400$ ka supra-Milankovitch cycle in a Fe-Mn crust

R. Banerjee et al.

---

Title Page

Abstract

Introduction

Conclusions

References

Tables

Figures



Back

Close

Full Screen / Esc

Printer-friendly Version

Interactive Discussion



sediments (Craig et al., 1993).

The Mg contents in our crust are suggested to have derived from high productivity of chlorophyll-*a*, which reaches at the maximum during periods of high primary productivity at certain geological time. Studies also suggested that there is direct impact of the insolation on equatorial productivity explaining the link between Southern Oscillation and intensity of zonal winds, which leads to the higher productivity of the surface waters in the equatorial Indian Ocean (Cayre et al., 1999). The record of high productivity in the surface water, during the growth history of this crust is also supported by the records of numerous planktonic foraminiferal tests entrapped within different microlayers of the crust, visible in the polished crust sections under reflected light microscope.

Planktonic uptake of essential metals and micronutrients, which are extremely low in concentrations in the surface seawater, get concentrated in their test, and after their death the trace metals get released in the deeper water (Morel and Price, 2003). Rickaby et al. (2007) studied periods of high Sr/Ca and high bloom production of *Gephyrocapsa caribbeanica* and *Emiliana huxleyi* in the SW Indian Ocean. They found the marked periods of high coccolithophore production are inversely correlated with the low amplitude 100- and 400-ka eccentricity cycles, and suggested a link between the production of coccolithophore blooms and eccentricity due to orbital control of silica leakage from the Southern Ocean. They further opined that the orbitally defined inverse correlation between insolation and growing season length result into the asymptotic growth response, and proposed a possible mechanism to account for the secular coccolithophore production cycles link with the 400-ka eccentricity forcing. Studies suggested that periodic changes in the cometary dust flux arrives through regular disturbances of the Oort clouds by variation in gravitational perturbation of Jupiter, Saturn and other extra-jovian planets, in addition to Galactic tides due to Galactic perturbations (Napier, 2001) which resulted into waves of extinction through dust and meteoritic impact. Changes in Na, Ni and Co contents at the 400-ka cycles in our crust record may be attributed to the cosmic/cometary dust flux in the ocean, which are transported into deep sea floor by the biological productivity of the ocean, incidentally reported at

**A ~400 ka  
supra-Milankovitch  
cycle in a Fe-Mn crust**

R. Banerjee et al.

Title Page

Abstract

Introduction

Conclusions

References

Tables

Figures



Back

Close

Full Screen / Esc

Printer-friendly Version

Interactive Discussion





the eccentricity levels (Johnson, 1998).

The 400 ka cycle recorded here in the Na, Mg, Ni and Co contents has been reported earlier in the Indian Ocean in radiolarian based SSTs (Gupta et al., 1996) and  $\delta-^{18}\text{O}$  records in foraminifers (Clemens and Tiedermann, 1997; Muller and Macdonald, 1997a,b), are attributed to the Earth's eccentricity cycles. Earlier, solar insolation cycles at 100, 41, and 23 ka are reported to have a major control on equatorial Indian Ocean primary production (Beaufort et al., 1997; Gupta et al., 2002; Gupta, 2003). Therefore, we calculated equatorial solar insolation during summer (21 April–21 July) using astronomical equation (Berger, 1978) in Analyseries (Paillard et al., 1996) at 25 ka ( $\delta t$ ) eliminating influence of precession signal, which is a product of the eccentricity ( $p=e\sin\omega$ ,  $e$ =eccentricity and  $\omega$ =the longitude of Sun's perihelion at given time, Berger, 1978; Berger and Loutre, 1992), for the last 3.5 Ma. MTM analysis of this summer insolation suggested cycles at  $\sim 400$ ,  $\sim 126$ ,  $\sim 95$  and  $\sim 54$ ,  $\sim 41$  and  $\sim 31$  ka (Fig. 6a), which are fundamental cycles due to the Earth's orbital eccentricity and the axial tilt, respectively (Berger, 1978). As our elemental data revealed only  $\sim 400$  ka cycle, we re-constructed the  $\sim 400$  ka insolation cycle, and compared it with the insolation data (Fig. 6b).

However, still the low frequency cycles like 41-ka tilt (less influence at equator than at pole, Berger and Loutre, 1992), if sampled at coarser time interval, may produce the lower frequency cycles like 100-, and 400-ka eccentricity due to aliasing effect. Hence, in order to rule out any artifact of aliasing in our reporting, we also calculated equatorial insolation at the same  $\delta t$  (110 ka) comparable at our average sampling interval in elemental data, by the precession (23-ka), tilt (41-ka) and 100-ka (eccentricity) signals to produce an artifact of 400-ka cycle. MTM power spectrum analysis at a high resolution, assuming normal signal (either), 50% reshaping, normalized and raw noise with log-fit criterion (misfit), of the summer insolation at  $\delta 110$ -ka suggested cycles at  $\sim 625$ -,  $\sim 425$ -, and 350-ka (Fig. 7a). Among them  $\sim 425$ -ka is the one of the fundamental cycle due to the Earth's orbital eccentricity (Berger, 1978). As our elemental data revealed only  $\sim 400$  ka cycle, we re-constructed the  $\sim 400$  ka insolation cycle, and

## A $\sim 400$ ka supra-Milankovitch cycle in a Fe-Mn crust

R. Banerjee et al.

Title Page

Abstract

Introduction

Conclusions

References

Tables

Figures



Back

Close

Full Screen / Esc

Printer-friendly Version

Interactive Discussion



compared it with the input insolation data (Fig. 7b). This comparison suggest that even though the  $\delta 110$ -ka sampling interval in elemental data is higher, it does not yield the aliased artifact result of the 400-ka eccentricity cycle.

Continuous Morlet wavelet transform (CMWT) analyses of power spectrum (Fig. 8) of Mg, Ni, and Co was performed following the method as described by Torrence and Compo (1998). In these analyses, the contour levels are chosen so that 75%, 50%, 25%, and 5% of the wavelet power is above each level, respectively. A zero padding is used to identify reduced variance and 20% significance level is identified by using a red-noise (autoregressive lag<sup>1</sup>) background spectrum. Results of this method suggested the existence of  $\sim 400$ -ka supra Milankovitch eccentricity related cycles in these three elements. However, they exhibited variation in the strenth of their power spectrum through time, suggesting that the 400-ka cycle is not uniformly strong throughtout the time.

The results thus suggested that, although the insolation variance of  $\sim 400$  ka eccentricity cycle is  $\sim 1/10$ th of the 100-ka eccentricity cycle, it was significant to cause notable changes in the ocean hydrochemistry generating  $\sim 400$  ka cycle due to eccentricity related solar insolation changes, as recorded in our Fe-Mn crust from Vityaz fracture zone.

## 4 Conclusions

We report here for the first time the longest geological record of  $\sim 3.5$  Ma with the  $\sim 400$  ka cycle in the Na, Mg, Pb, Ni, and Co contents in a hydrogenous Fe-Mn crust, collected from abyssal depth of the equatorial Indian Ocean. Fe-Mn crusts are very good repository of long term ocean productivity cycles, due to the result of the geochemical response to the Earth's eccentricity cycle ( $\sim 400$  ka) related solar insolation changes. Our finding of  $\sim 400$  ka supra-Milankovitch cycle from equatorial Indian Ocean corroborated with the previously reported  $\sim 400$  ka cycle due to eccentricity. In our data, although the amplitude of insolation at  $\sim 400$  ka cycle is very small (1/10th)

CPD

6, 1311–1335, 2010

## A $\sim 400$ ka supra-Milankovitch cycle in a Fe-Mn crust

R. Banerjee et al.

Title Page

Abstract

Introduction

Conclusions

References

Tables

Figures

◀

▶

◀

▶

Back

Close

Full Screen / Esc

Printer-friendly Version

Interactive Discussion



compared to the 41 ka tilt cycle, it is still significant to yield considerable changes in geological record, preserved in the elemental contents of the Fe-Mn crust. Very good correlation between the  $^{230}\text{Th}_{\text{excess}}$  based dates and Co-chronometric dates for the top 0–8 mm of the crust ( $r=0.9734$ , at 99.9% significance level) and assuming the similar relationship might have existed in the past in samplers older than 0.5 Ma our age model is reasonably sound.

*Acknowledgements.* Authors thank to DOD and CSIR, New Delhi for ship time and logistic support. RB is thankful to INSA, New Delhi and JSPS, Tokyo for a fellowship to visit Hokkaido University, where part of the analytical work was carried out. This work is partially funded by US-INDIA Fund through ONR (Grant # 0014-97-1-0925). M. Shyam Prasad and V.P.C. Rao are thanked for suggestions to improve the presentation. This work is carried out as part of N.I.O's on going Project GAP 2175 on "Deep-sea mineral exploration". This is N.I.O's contribution no. 4802.

## References

- Banakar, V. K. and Borole, D. V.: Depth profiles of  $^{230}\text{Th}_{\text{excess}}$ , transition metals and mineralogy of the ferromanganese crusts of the central Indian Ocean basin and implications for paleoceanographic influence on crust genesis, *Chem. Geol.*, 94, 33–44, 1991.
- Banerjee, R., Roy, S., Dasgupta, S., Mukhopadhyay, S., and Miura, H.: Petrogenesis of ferromanganese nodules from east of the Chagos Archipelago, central Indian Basin, *Indian Ocean, Mar. Geol.*, 157, 145–148, 1999.
- Beaufort, L., Lancelot, Y., Camberlin, P., Cayre, O., Vincent, E., Bassinot, F., and Labeyrie, L.: Insolation cycles as a major control of equatorial Indian Ocean primary production, *Science*, 278, 1451–1454, 1997.
- Berger, A. L.: Support for the astronomical theory of climatic change, *Nature*, 269, 44–45, 1977.
- Berger, A. L.: Long term variations of daily insulations and quaternary climatic changes, *J. Atmos. Sci.*, 35, 2362–2367, 1978.
- Berger, A. L. and Loutre, M. F.: Astronomical solutions for paleoclimatic studies over the last 3 Million years, *Earth Planet. Sc. Lett.*, 111, 369–382, 1992.

## A ~400 ka supra-Milankovitch cycle in a Fe-Mn crust

R. Banerjee et al.

Title Page

Abstract

Introduction

Conclusions

References

Tables

Figures

◀

▶

◀

▶

Back

Close

Full Screen / Esc

Printer-friendly Version

Interactive Discussion



---

**A ~400 ka  
supra-Milankovitch  
cycle in a Fe-Mn crust**R. Banerjee et al.

---

[Title Page](#)[Abstract](#)[Introduction](#)[Conclusions](#)[References](#)[Tables](#)[Figures](#)[Back](#)[Close](#)[Full Screen / Esc](#)[Printer-friendly Version](#)[Interactive Discussion](#)

Berger, W. H., Smetacek, V. S., and Wefer, G.: Ocean productivity and paleoproductivity – an overview, in: *Productivity of the Ocean: Present and Past*, edited by: Berger, W. H., Smetacek, V. S., and Wefer, G., Wiley and Sons, New York, USA, 1–34, 1989.

Cayre, O., Beaufort, L., and Vincent, E.: Paleoproductivity in the Equatorial Indian Ocean for the last 260 000 yr: a transfer function based on planktonic foraminifera, *Quat. Sci. Rev.*, 18, 839–857, 1999.

Clemens, S. C.: Dust response to seasonal atmospheric forcing: proxy evaluation and calibration, *Paleoceanography*, 13, 471–490, 1998.

Clemens, S. C., and Tiedemann, R.: Eccentricity forcing of Pliocene–Early Pleistocene climate revealed in a marine oxygen-isotope record, *Nature*, 385, 801–804, 1997.

Craig R. G., Kroon, D., and Wei, W.: Sedimentary rhythms and climatic forcing of Pleistocene–Holocene mixed carbonate/silici-carbonate sediments off the Great Barrier Reef, in: *Proceedings of the Ocean Drilling Program, Scientific Results*, National Science foundation, edited by: McKenzie, J. A. Davies, P.J., Palmer-Julson, A., et al., Washington, DC, 133, 189–202, 1993.

DeMenocal, P. B.: Plio-pleistocene African climate, *Science*, 270, 53–59, 1995.

DeMets, C. and Royer, J. Y.: A new high-resolution model for India-Capricorn motion since 20 Ma: implications for the chronology and magnitude of distributed crustal deformation in the central Indian basin, *Curr. Sci.*, 85, 339–345, 2003.

Edwards, M. A. and Harrison, T. M.: When did the roof collapse? Late miocene north-south extension in the high Himalaya revealed by Th-Pb monazite dating of the Khula Kangri Granite, *Geology*, 25, 543–546, 1997.

Frank, M., O’Nions, R. K., Hein, J. R., and Banakar, V. K.: 60 Ma records of major elements and Pb-Nd isotopes from hydrogenous ferromanganese crusts: reconstruction of seawater paleochemistry, *Geochim. Cosmochim. Ac.*, 63, 11/12, 1689–1708, 1999.

Ghil, M., Allen, M. R., Dettinger, M. D., Ide, K., Kondrashov, D., Mann, M. E., Robertson, A. W., Saunders, A., Tian, Y., Varadi, F., and Yiou, P.: Advanced spectral methods for climatic time series, *Rev. Geophys.*, 40, 1–23, 2001.

Guptha M. V. S., Banerjee, R., and Lina, M.: On the nature of the calcareous substrate of a ferromanganese crust from the Vityaz Fracture Zone, central Indian Ridge: inferences on paleoceanography, *Geo-Mar. Lett.*, 22, 2–18, 2002.

Gupta, S. M.: Pyloniid stratigraphy – a new tool to date tropical radiolarian ooze from the central tropical Indian Ocean, *Mar. Geol.*, 184, 85–93, 2002.

- Gupta, S. M.: Orbital frequencies in radiolarian assemblages of the central Indian Ocean: implications on the Indian summer monsoon, *Palaeogeol. Palaeoclimatol. Palaeoecol.*, 197, 97–112, 2003.
- Gupta, S. M., Fernandes, A. A., and Mohan, R.: Tropical sea surface temperatures and the Earth's eccentricity cycle, *Geophys. Res. Lett.*, 23, 3159–3162, 1996.
- Han, X., Jin, X., Yang, S., Fietzke, J., and Eisenhauer, A.: Rhythmic growth of Pacific ferromanganese nodules and their Milankovitch climatic origin, *Earth Planet. Sc. Lett.*, 211, 143–157, 2003.
- Hays, J. D., Imbrie, J., and Shackleton, N.: Variations in the Earth's orbit: pacemaker of the Ice-Ages, *Science*, 194, 1121–1132, 1976.
- Heegaard, E., Birks, H. J. B., and Telford, R. J.: Relationships between calibrated ages and depth in stratigraphical sequences: an estimation procedure by mixed-effect regression, *Holocene*, 15, 612–618, 2005.
- Hein, J. R., Bohrsen, W. A., Schulz, M. S., Noble, M., and Clague, D.: Variations in the fine-scale compositions of a Central Pacific ferromanganese crust: paleoceanographic implications, *Palaeoceanography*, 7, 63–77, 1992.
- Herzig, P. M. and Plüger, W. L.: Explorations for hydrothermal activity near the Rodriguez Triple Junction, Indian Ocean, *Can. Mineral.*, 26, 721–736, 1988.
- Hyun, S., Naokaze A., and Ho-Il, Y. : Milankovitch cycles and paleoceanographic evolution within sediments from ODP Sites 980 and 983 of the North Atlantic Ocean, *Geosci. J.*, 9, 235–242, 2005.
- Johnson, K. S.: Iron supply and demand in the upper ocean: is extraterrestrial dust a significant source of bioavailable iron, *Global Biogeochem. Cy.*, 15, 61–63, 2001.
- Jeong, K. S., Jung, H. S., Kang, J. K., Morgan, C. L., and Hein, J. R.: Formation of ferromanganese crusts on northwest intertropical Pacific seamounts: electron photomicrography and microprobe chemistry, *Mar. Geol.*, 162, 541–559, 2000.
- Klemm, V., Levasseur, S., Frank, M., Hein, J. R., and Halliday, H. N.: Osmium isotope stratigraphy of a marine ferromanganese crust, *Earth Planet. Sc. Lett.*, 238, 42–48, 2005.
- Koide, M., Bruland, K. W., and Goldberg, E. D.:  $^{228}\text{Th}/^{232}\text{Th}$  and  $^{210}\text{Pb}$  geochronologies in marine and lake sediments, *Geochim. Cosmochim. Ac.*, 37, 1171–1187, 1973.
- Krishnaswami, S. and Lal, D.: Radionuclide limnology, in: *Lakes, Chemistry, Geology, Physics*, edited by: Lerman, A., Springer Verlag, New York, USA, 153–177, 1978.
- Krishnaswami, S. and Sarin, M. M.: Procedures for simultaneous determination of the Th, Pu,

---

## A ~400 ka supra-Milankovitch cycle in a Fe-Mn crust

R. Banerjee et al.

---

Title Page

Abstract

Introduction

Conclusions

References

Tables

Figures

◀

▶

◀

▶

Back

Close

Full Screen / Esc

Printer-friendly Version

Interactive Discussion





- on electron microprobe analysis (EMPA), *Mar. Geophys. Res.*, 28, 165–182, 2007.
- Rickaby, R. E. M., Bard, E., Sonzogni, C., Rostek, F., Beaufort, L., Barker, S., Rees, G., and Schrag, D. P.: Coccolith chemistry reveals secular variations in the global ocean carbon cycle?, *Earth Planet. Sc. Lett.*, 253, 83–95, 2007.
- 5 Royer, J. Y., Gordon, R. G., DeMets, C., and Vogt, P. R.: New limits on the motion between India and Australia since chron 5 (11 Ma) and implications for lithospheric deformation in the equatorial Indian Ocean, *Geophys. J. Int.*, 129, 41–74, 1997.
- Schulz, M. and Mudelsee, M.: REDFIT: estimating red-noise spectra directly from unevenly spaced paleoclimatic time series, *Comp. Geosci.*, 28, 421–426, 2002.
- 10 Thomson, D. J.: Spectrum estimation and harmonic analysis, *Proc. IEEE*, 70, 1055–1096, 1982.
- Thomson, D. J.: Quadratic-inverse spectrum estimates: applications to palaeoclimatology, *Philos. T. R. Soc. Lond. A*, 332, 539–597, 1990.
- Tiedemann, R. M., Sarnthein, M., and Shackleton, N. J.: Astronomic timescale for the pliocene Atlantic  $\delta^{18}\text{O}$  and dust flux records from Ocean Drilling Program Site 659, *Paleoceanography*, 9, 619–638, 1994.
- 15 Torrence, C. and Compo, G. P.: A practical guide to wavelet analysis, *B. Am. Meteorol. Soc.*, 79, 61–78, 1998.

---

## A ~400 ka supra-Milankovitch cycle in a Fe-Mn crust

R. Banerjee et al.

---

Title Page

Abstract

Introduction

Conclusions

References

Tables

Figures

◀

▶

◀

▶

Back

Close

Full Screen / Esc

Printer-friendly Version

Interactive Discussion



**Table 1.** Elemental concentration (%) of the crust at each millimeter depth level. Growth rate (GR) in mm. Ma<sup>-1</sup> of each level was calculated by “cobalt chronometer” method (Manheim and Lane-Bostwick, 1988).

Depth	Mg	Na	Al	Si	Ca	Ti	Mn	Fe	Ni	Cu	Co	Zn	Sr	Ba	Pb	GR	age (Ma)
0–1	1.5	1.2	0.4	4.3	2.3	0.6	19.0	27.8	0.2	0.1	0.1	0.1	0.2	0.1	0.6	22.66	0.04
1–2	1.9	0.7	0.3	4.9	2.9	0.7	15.1	33.1	0.2	0.1	0.2	0.1	0.2	0.2	0.1	17	0.09
2–3	1.2	0.7	0.3	4.2	2.6	0.7	17.9	30.3	0.2	0.0	0.2	0.1	0.2	0.1	0.5	11.33	0.17
3–4	1.0	0.5	0.3	3.1	2.7	0.8	17.4	24.2	0.2	0.1	0.3	0.1	0.2	0.1	0.0	4.85	0.37
4–5	1.3	0.6	0.4	4.9	2.3	0.6	16.6	31.1	0.2	0.1	0.3	0.1	0.2	0.1	0.2	6.18	0.53
5–6	1.4	0.9	0.3	3.3	1.7	0.6	18.4	25.7	0.2	0.0	0.2	0.0	0.2	0.2	0.6	11.33	0.61
6–7	1.3	0.7	0.3	4.0	3.1	0.7	19.6	30.5	0.2	0.1	0.1	0.1	0.2	0.1	0.0	22.66	0.65
7–8	1.0	1.1	0.3	3.9	2.7	0.5	20.4	30.4	0.2	0.1	0.1	0.1	0.2	0.2	0.7	34	0.67
8–9	1.4	1.2	0.3	4.0	3.5	0.7	17.9	31.2	0.2	0.1	0.2	0.1	0.2	0.2	0.5	13.6	0.74
9–10	1.4	0.6	0.3	3.5	1.8	0.5	18.5	28.6	0.2	0.1	0.2	0.0	0.2	0.2	0.2	17	0.79
10–11	1.3	0.7	0.4	3.4	2.0	0.4	16.6	26.8	0.2	0.1	0.1	0.1	0.2	0.2	0.3	17	0.84
11–12	1.5	1.1	0.4	3.2	3.4	0.7	20.8	25.8	0.3	0.1	0.2	0.1	0.2	0.1	0.5	13.6	0.91
12–13	1.2	0.4	0.5	4.1	2.6	0.6	18.7	30.8	0.2	0.1	0.2	0.1	0.2	0.1	0.4	17	0.96
13–14	1.4	0.7	0.5	3.1	3.4	0.8	23.8	26.5	0.4	0.1	0.3	0.1	0.2	0.1	0.2	7.55	1.03
14–15	1.4	0.9	0.6	2.9	3.5	0.7	23.1	25.2	0.4	0.2	0.2	0.1	0.2	0.2	0.2	9.71	1.13
15–16	1.1	0.5	0.7	2.7	2.0	0.6	19.1	29.8	0.3	0.1	0.2	0.1	0.2	0.1	1.0	13.6	1.2
16–17	1.2	1.4	0.7	4.3	2.3	0.6	17.1	28.6	0.1	0.1	0.1	0.1	0.2	0.1	0.2	22.66	1.24
17–18	1.1	0.9	0.8	5.0	2.3	0.7	16.5	30.8	0.1	0.1	0.1	0.1	0.2	0.2	0.5	34	1.26
18–19	1.4	0.6	0.9	5.1	2.3	0.8	16.8	30.8	0.2	0.1	0.2	0.1	0.2	0.1	0.4	11.33	1.34
19–20	1.4	0.5	0.8	4.0	1.4	0.8	18.0	29.0	0.3	0.1	0.2	0.1	0.2	0.1	0.6	8.5	1.45
20–21	1.4	1.1	1.0	4.6	2.7	0.8	18.6	29.7	0.2	0.1	0.2	0.1	0.2	0.1	0.5	9.71	1.55
21–22	1.2	0.7	0.8	4.6	2.8	0.6	17.5	30.5	0.1	0.1	0.1	0.1	0.2	0.1	0.6	68	1.56
22–23	1.6	1.1	0.9	4.5	3.1	0.5	18.1	28.4	0.2	0.1	0.2	0.1	0.2	0.1	0.4	9.71	1.66
23–24	1.3	0.6	0.9	4.9	2.2	0.6	17.4	31.0	0.2	0.1	0.3	0.1	0.2	0.2	0.5	6.18	1.82
24–25	1.2	1.1	1.0	4.9	3.0	1.1	16.5	31.9	0.2	0.1	0.2	0.0	0.2	0.2	0.5	7.55	1.95
25–26	1.4	0.7	0.8	3.8	2.9	0.8	18.0	27.1	0.3	0.1	0.2	0.1	0.2	0.1	0.7	13.6	2.02
26–27	1.4	0.3	1.0	3.8	3.2	0.9	18.5	27.7	0.3	0.1	0.3	0.1	0.2	0.1	0.2	4.85	2.22
27–28	1.3	0.4	1.0	4.6	2.1	0.8	15.1	31.9	0.2	0.1	0.4	0.1	0.2	0.2	0.4	3.57	2.50
28–29	1.4	0.5	0.9	4.1	3.6	1.0	18.2	29.4	0.3	0.1	0.3	0.1	0.2	0.1	0.3	5.66	2.67
29–30	1.5	0.5	1.1	4.4	3.5	1.1	17.3	30.0	0.2	0.1	0.3	0.1	0.2	0.2	0.4	4.85	2.87
30–31	1.5	0.5	1.0	4.0	3.2	1.1	18.1	28.2	0.3	0.1	0.3	0.1	0.2	0.2	0.0	4	3.12
31–32	1.2	0.4	1.3	3.4	2.4	0.9	10.4	17.1	0.4	0.2	0.2	0.1	0.1	0.1	0.4	3.09	3.52

**A ~400 ka  
supra-Milankovitch  
cycle in a Fe-Mn crust**

R. Banerjee et al.

Title Page

Abstract Introduction

Conclusions References

Tables Figures

◀ ▶

◀ ▶

Back Close

Full Screen / Esc

Printer-friendly Version

Interactive Discussion





## A ~400 ka supra-Milankovitch cycle in a Fe-Mn crust

R. Banerjee et al.

**Table 2.** Details of radiometric analysis of the top 8 mm of the crust by  $^{230}\text{Th}_{\text{excess}}$  method, including layer by layer age and their error limits .

Depth (mm)	$^{210}\text{Pb}$ dpm/g	$^{230}\text{Th}$ dpm/g	$^{230}\text{Th}_{\text{exc}}$ dpm/g	Age (Ma)
0.25	86.27±4.09	304.55±11.14	299.62±11.14	0.04±0.00
0.75	24.66±1.30	100.56±4.30	95.64±4.31	0.13±0.01
1.5	14.75±1.22	31.86±1.42	26.94±1.45	0.25±0.01
2.5	12.27±0.87	13.62±0.88	8.70±0.93	0.42±0.02
3.5	10.15±0.63	9.79±0.62	4.86±0.69	0.47±0.11
4.5	10.62±1.03	9.78±0.59	4.86±0.67	0.53±0.09
5.5	9.98±0.97	12.35±1.26	7.42±1.30	0.61±0.11
6.5	11.98±0.96	9.05±0.55	4.13±0.62	0.70±0.14
7.5	10.46±0.73	8.53±0.50	3.61±0.59	0.80±0.19

Title Page

Abstract

Introduction

Conclusions

References

Tables

Figures

◀

▶

◀

▶

Back

Close

Full Screen / Esc

Printer-friendly Version

Interactive Discussion



## A ~400 ka supra-Milankovitch cycle in a Fe-Mn crust

R. Banerjee et al.

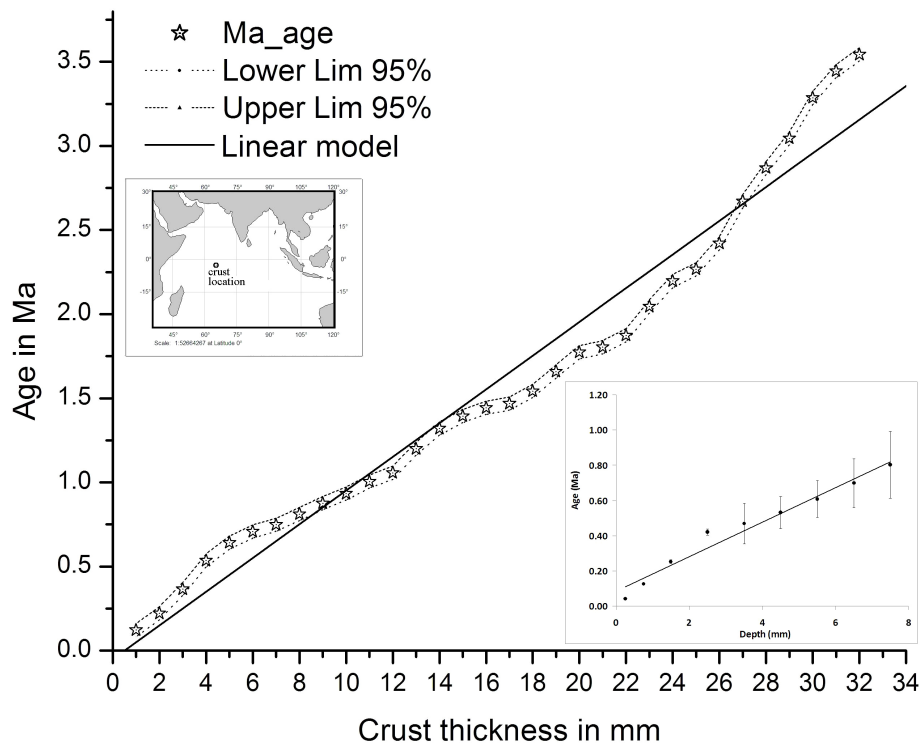


**Fig. 1.** Location of the crust in the equatorial Indian Ocean (left inset),  $^{230}\text{Th}_{\text{excess}}$  vs. crust depth (right inset), and the Co-chronometric dates based age Vs depth in age model.

Title Page

Abstract

Introduction

Conclusions

References

Tables

Figures

◀

▶

◀

▶

Back

Close

Full Screen / Esc

Printer-friendly Version

Interactive Discussion

**A ~400 ka  
supra-Milankovitch  
cycle in a Fe-Mn crust**

R. Banerjee et al.

Title Page

Abstract

Introduction

Conclusions

References

Tables

Figures

◀

▶

◀

▶

Back

Close

Full Screen / Esc

Printer-friendly Version

Interactive Discussion

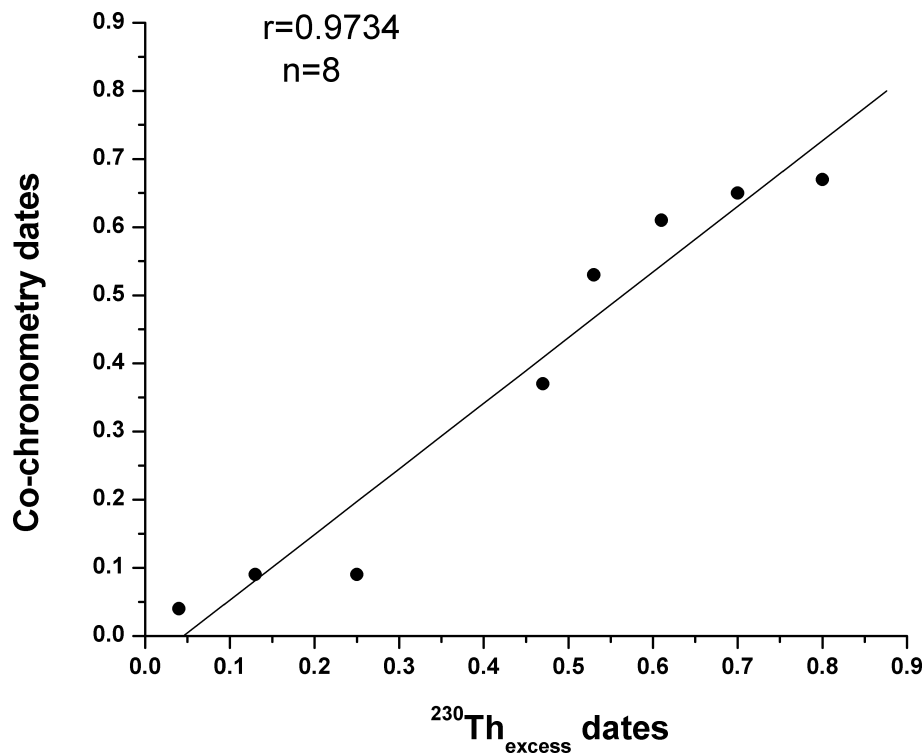


**Fig. 2.** Correlation between  $^{230}\text{Th}_{\text{excess}}$  dates and Co-chronometric dates (in Ma) of crust in top 0–8 mm layer.

## A ~400 ka supra-Milankovitch cycle in a Fe-Mn crust

R. Banerjee et al.

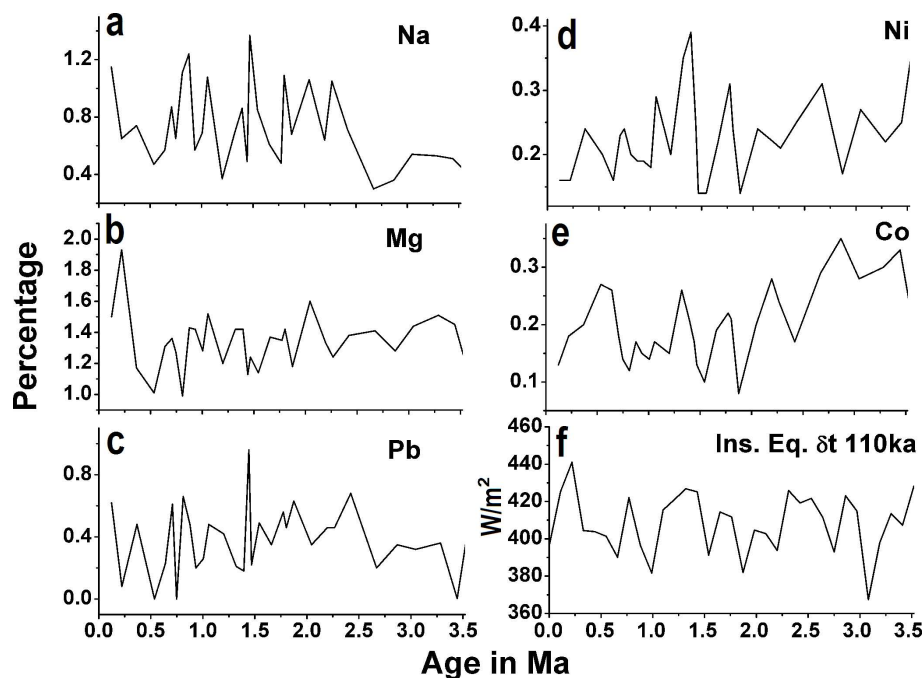


**Fig. 3.** Time series of Na (a), Mg (b), Pb (c), Ni (d), Co (e) contents against Co-chronometric dates based age model in the crust, and the equatorial insolation from 21 April–21 July at  $\delta t=110$ -ka (f) in the last 3.5 Ma.

Title Page

Abstract

Introduction

Conclusions

References

Tables

Figures

◀

▶

◀

▶

Back

Close

Full Screen / Esc

Printer-friendly Version

Interactive Discussion



## A ~400 ka supra-Milankovitch cycle in a Fe-Mn crust

R. Banerjee et al.

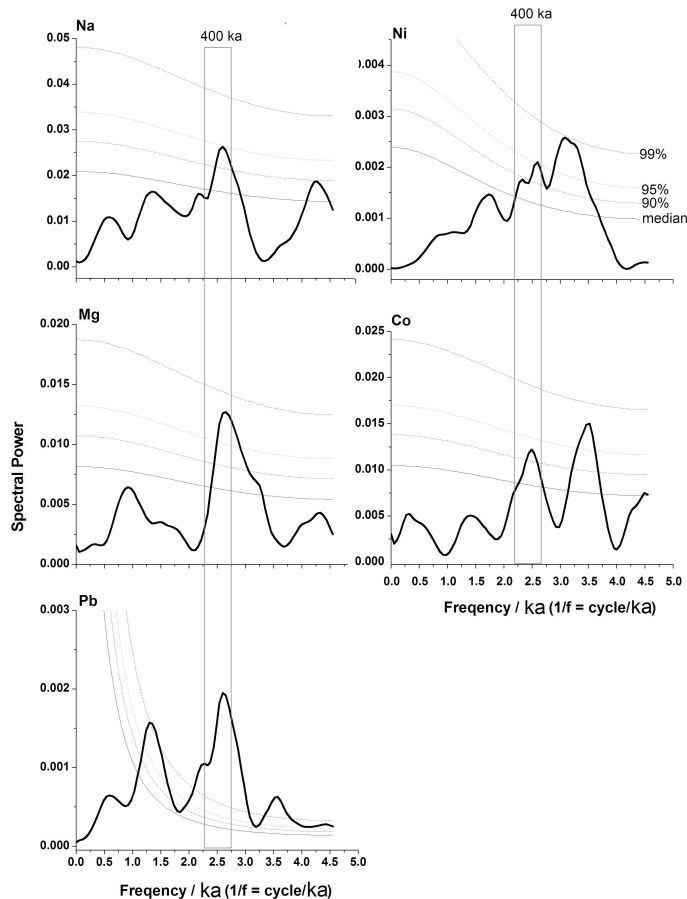


**Fig. 4.** Red-Fit spectral results exhibiting significant ~400 ka eccentricity cycles at >90–99% significance levels

Title Page

Abstract

Introduction

Conclusions

References

Tables

Figures

◀

▶

◀

▶

Back

Close

Full Screen / Esc

Printer-friendly Version

Interactive Discussion



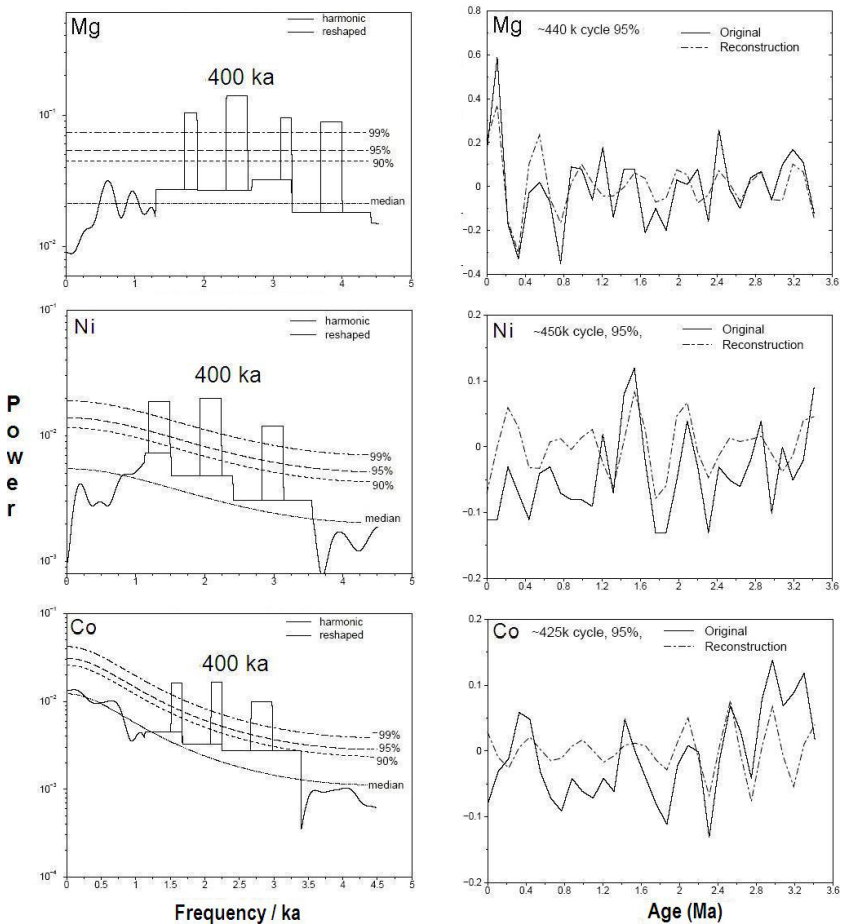


**Fig. 5.** MTM spectrum of Mg, Ni and Co (left panel) showing ~400 ka cycle and the cyclic component along with original time series (right panel).

**A ~400 ka supra-Milankovitch cycle in a Fe-Mn crust**

R. Banerjee et al.

Title Page

Abstract Introduction

Conclusions References

Tables Figures

◀ ▶

◀ ▶

Back Close

Full Screen / Esc

Printer-friendly Version

Interactive Discussion



## A ~400 ka supra-Milankovitch cycle in a Fe-Mn crust

R. Banerjee et al.

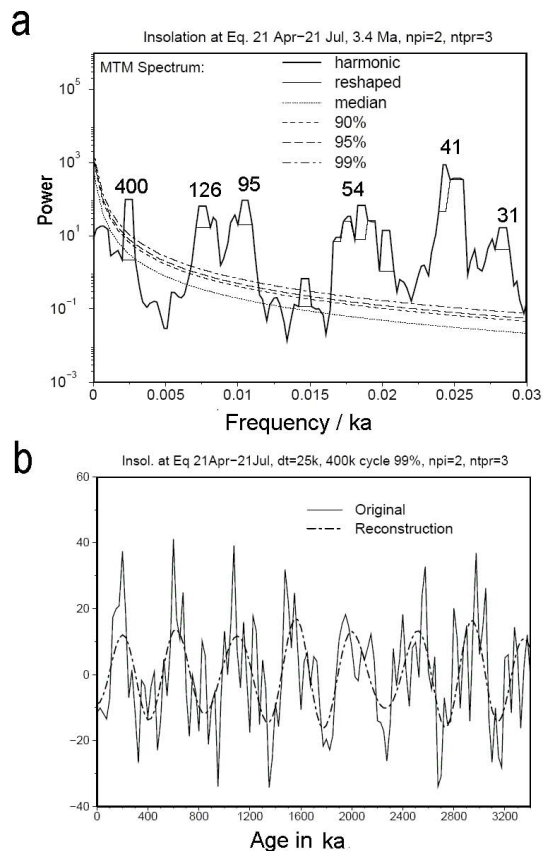


**Fig. 6.** (a) MTM spectrum of equatorial summer insolation (Berger, 1978) with emphasis on low frequency band exhibiting significant cycles at ~400, 126, 95, 54, 41 and 31 ka. (b) Comparison between the reconstructed ~400 ka cyclic component and the insolation time series.

Title Page

Abstract

Introduction

Conclusions

References

Tables

Figures

◀

▶

◀

▶

Back

Close

Full Screen / Esc

Printer-friendly Version

Interactive Discussion



## A ~400 ka supra-Milankovitch cycle in a Fe-Mn crust

R. Banerjee et al.

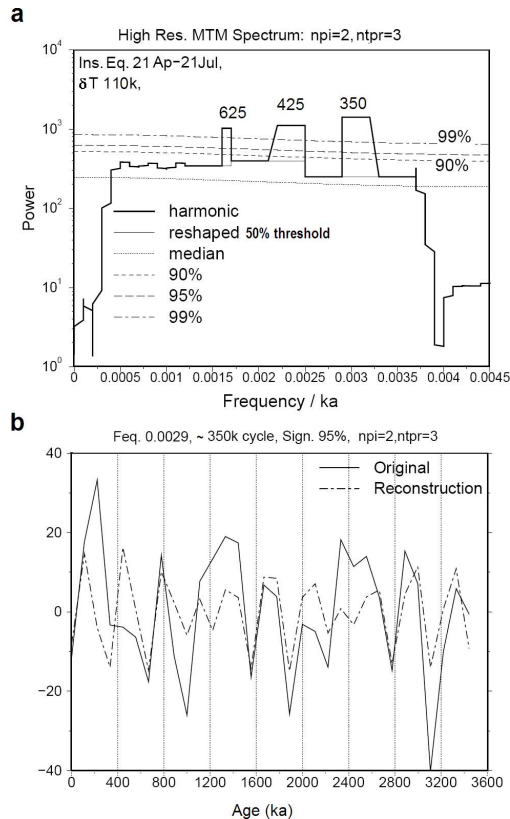


**Fig. 7. (a)** MTM spectrum of equatorial summer insolation (Berger, 1978) at  $\delta t=110$ -ka with emphasis on low frequency band exhibiting significant cycles at ~625-, ~425-, and ~350-ka. Perhaps, ~400-ka cycle is bilobed into ~425- and ~350-ka, but ruling out any aliasing by large sampling of low period precession (23-ka), tilt (41-ka) and eccentricity (100-ka) cycles. **(b)** Comparison between the reconstructed ~400 ka cyclic component and the insolation time series.



## A ~400 ka supra-Milankovitch cycle in a Fe-Mn crust

R. Banerjee et al.

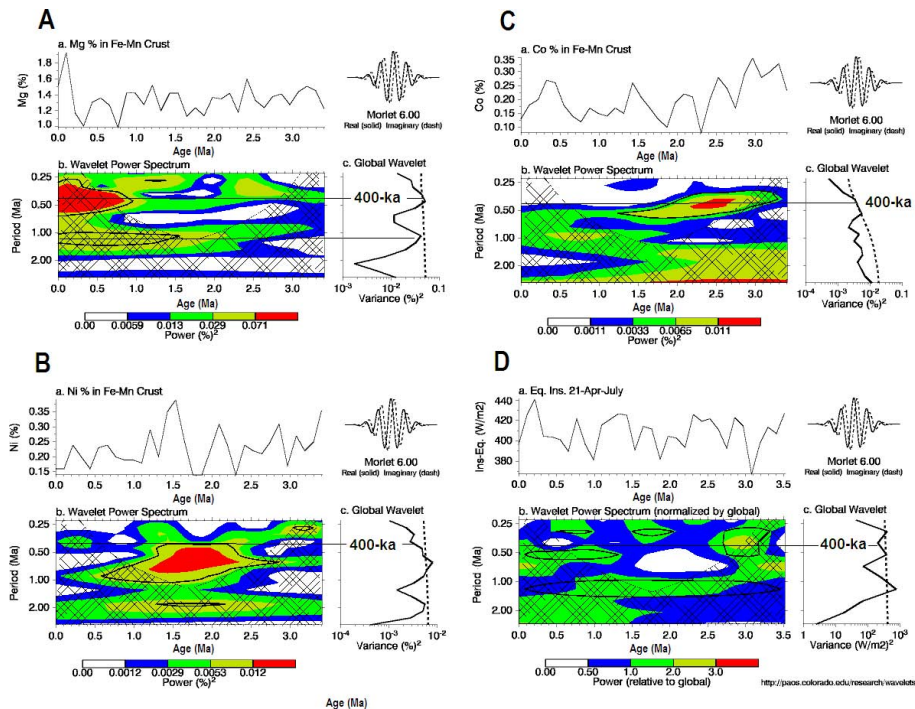


**Fig. 8.** Continuous wavelet (Morlet) transform analyses of Mg (**A**), Ni (**B**), Co (**C**), and insolation at equator with  $\delta t$  110-ka (**D**) showing presence of ~400-ka cycles with variation in their strength of power through time. **(a)** Elemental % in the crust. **(b)** The wavelet power spectrum. The contour levels are chosen so that 75%, 50%, 25%, and 5% of the wavelet power is above each level, respectively. The cross-hatched region is the cone of influence, where zero padding has reduced the variance. Black contour is the 20% significance level, using a red-noise (autoregressive lag<sup>1</sup>) background spectrum. **(c)** The global wavelet power spectrum (black line). The dashed line is the significance for the global wavelet spectrum, assuming the same significance level and background spectrum as in **(b)**.